

# Comparative Metabolomics and Microbiome Analysis of Ethanol versus OMNImet/gene•GUT Fecal Stabilization

Heidi Isokääntä, Lucas Pinto da Silva, Naama Karu, Teemu Kallonen, Anna-Katariina Aatsinki, Thomas Hankemeier, Leyla Schimmel, Edgar Diaz, Tuulia Hyötyläinen, Pieter C. Dorrestein, Rob Knight, Matej Orešič, Rima Kaddurah-Daouk,\* Alex M. Dickens,\* and Santosh Lamichhane\*



Cite This: *Anal. Chem.* 2024, 96, 8893–8904



Read Online

ACCESS |



Metrics & More

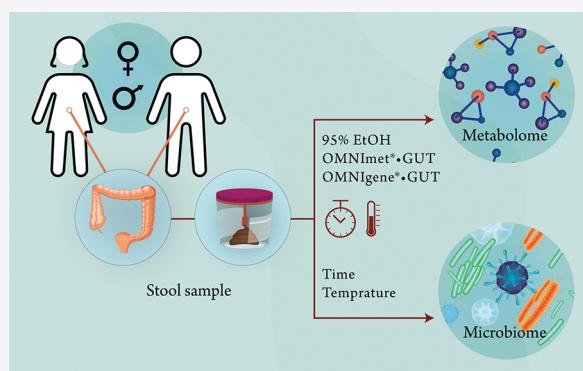


Article Recommendations



Supporting Information

**ABSTRACT:** Metabolites from feces provide important insights into the functionality of the gut microbiome. As immediate freezing is not always feasible in gut microbiome studies, there is a need for sampling protocols that provide the stability of the fecal metabolome and microbiome at room temperature (RT). Here, we investigated the stability of various metabolites and the microbiome (16S rRNA) in feces collected in 95% ethanol (EtOH) and commercially available sample collection kits with specific preservatives OMNImet•GUT/OMNIGene•GUT. To simulate field-collection scenarios, the samples were stored at different temperatures at varying durations (24 h + 4 °C, 24 h RT, 36 h RT, 48 h RT, and 7 days RT) and compared to aliquots immediately frozen at −80 °C. We applied several targeted and untargeted metabolomics platforms to measure lipids, polar metabolites, endocannabinoids, short-chain fatty acids (SCFAs), and bile acids (BAs). We found that SCFAs in the nonstabilized samples increased over time, while a stable profile was recorded in sample aliquots stored in 95% EtOH and OMNImet•GUT. When comparing the metabolite levels between aliquots stored at room temperature and at +4 °C, we detected several changes in microbial metabolites, including multiple BAs and SCFAs. Taken together, we found that storing samples at RT and stabilizing them in 95% EtOH yielded metabolomic results comparable to those from flash freezing. We also found that the overall composition of the microbiome did not vary significantly between different storage types. However, notable differences were observed in the  $\alpha$  diversity. Altogether, the stability of the metabolome and microbiome in 95% EtOH provided results similar to those of the validated commercial collection kits OMNImet•GUT and OMNIGene•GUT, respectively.



## THEORETICAL BACKGROUND

The gut microbiome is considered an “essential organ” that contributes to the regulation of host development and physiology and facilitates host metabolism<sup>1,2</sup> and is often linked to various human health conditions,<sup>3,4</sup> including inflammatory bowel disease,<sup>5</sup> obesity,<sup>6</sup> and multiple neurological disorders.<sup>7,8</sup> The interaction and dynamics between the host and gut microbiome are mediated by metabolites, which serve as vital signaling molecules.<sup>9</sup> Integrated microbiome and metabolome analyses have emerged as the foremost promising approach to unveil host–microbiota interactions in the context of disease risk.<sup>10</sup>

Over the past decade, fecal metabolomics has received increasing attention as fecal metabolites offer important insights into the functional aspects of the gut microbiome. The molecules associated with the gut microbiome also have the potential to be used in therapeutic strategies and biomarker discovery.<sup>11</sup> Despite growing interest, among the limiting factors in this field are practical challenges involved in the collection of human fecal samples. Albeit logistically

impractical, the immediate homogenization and freezing of fecal samples at −80 °C is considered the gold standard for metabolite preservation because it halts enzymatic activity, hydrolysis, oxidation, and other degradation processes.<sup>12</sup> Recently, studies of large human cohorts increased the demand for home collection of human fecal specimens, with the aim of reducing cost as well as improving practicality, donor privacy, and convenience. Although home collection is a convenient option, it includes multiple steps that can involve temperature fluctuations. Moreover, storing and shipping frozen fecal samples can be inconvenient for participants and prohibitively expensive for researchers. This emphasizes the need for sampling systems that can be stored at room temperature.<sup>13</sup>

**Received:** October 2, 2023

**Revised:** April 12, 2024

**Accepted:** April 18, 2024

**Published:** May 23, 2024



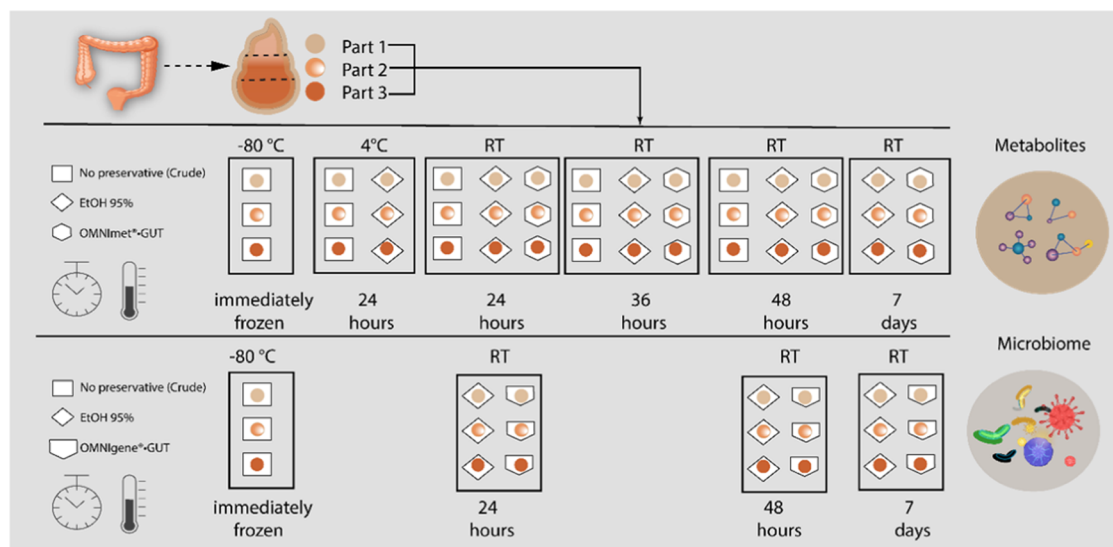


**Figure 1.** An overview of the study design is presented, illustrating the feces samples collected for metabolite measurement as well as the number of matched feces samples for 16S rRNA gene sequencing at each time point. In this study, one set of samples was frozen immediately ( $-80\text{ }^{\circ}\text{C}$ ) while other aliquots were either stored as crude feces (without preservatives), in 95% ethanol or in the OMNIgene•GUT/OMNIImet•GUT at room temperature (RT) for 24 h, 48 h, and 7 days.

To address this need specifically for metabolomics analysis, available sampling devices such as DNA stabilization tubes and fecal immunochemical test tubes were critically assessed.<sup>14,15</sup> These studies found that the numerous detergents, buffers, salts, and other additives in the examined collection tubes deemed them inferior or unsuitable for analysis by liquid chromatography (LC) and mass spectrometry (MS). In addition, some of these collection kits can significantly distort the metabolic profile of fecal samples compared to the gold standard of flash freezing.<sup>14,15</sup> A few studies tested 95% ethanol (EtOH) as a fecal sample preservative and found it suitable for metabolomics.<sup>10,15</sup> Ethanol prevents microbial growth and stabilizes the microbiome until profiling while partly stabilizing the metabolome, as it prevents enzymatic metabolism by the fecal microbiota and affects chemical degradation processes.<sup>16</sup> Another stability contributor effect of 95% EtOH is its nonfrozen state at  $-80\text{ }^{\circ}\text{C}$ ; hence, no freeze–thaw cycles occur and disrupt the sample profile. Fecal collection and storage tubes containing 95% EtOH (OMNIImet•GUT, DNA Genotek, Canada) have been introduced as a kit tailored specifically for metabolomics analysis. A corresponding kit for the microbiome (OMNIgene•GUT) has been used in several studies.<sup>17,18</sup> To our knowledge, only a few studies compared feces collection methods for simultaneous gut microbiota profiling and fecal metabolomics.<sup>10</sup> Notably, studies comparing collection with that of 95% EtOH and commercial fecal collection kits are lacking.

Here, we aim to fill the current knowledge gaps and establish the validity of an off-site fecal collection method that preserves the integrity of both the metabolome and the microbiome during the freight and until processing. For this goal, 95% ethanol was selected as a preservative and compared with flash freezing (crude feces without solvent), OMNIImet•GUT, and OMNIgene•GUT, which are validated commercial collection kits for fecal metabolome and microbiome profiling, respectively. We also tested the effect of different storage times and temperatures on metabolite coverage with EtOH-containing matrices in terms of their sensitivity, robustness, and throughput.

## EXPERIMENTAL SECTION

**Study Design.** Stool samples were collected from four healthy human volunteers ( $n = 4$ ) for metabolomics and microbiome profiling (Figure 1); informed consent was obtained from all donors. Fecal samples were collected from the four subjects in the morning next to the operating laboratory. After defecation, the sample was divided into three parts, which were homogenized with a spatula. These represent biological replicates, and they were further divided into aliquots.

For the metabolomics analyses, the aliquot tubes were spiked with stability standards (sodium butyrate-13C4 5 ppm, cholic acid-24-13C 2,5 ppb, palmitic acid (1-13C, 99%) 5 ppm, hippuric acid-d5 5 ppm, indole-2,4,5,6,7-d5-3-acetic acid 5 ppm, nicotinamide-d4 5 ppm, sucrose-1-13Cfr 5 ppm, L-tyrosine-d4 5 ppm, and cortisol-1,2-d2 5 ppm) and dried using a SpeedVac (Thermo Fisher Scientific) beforehand. For the aliquots,  $150 \pm 10$  mg of stool was weighed to each prepared tube. Next, storage fluid was added at a ratio of 1:4 (600  $\mu\text{L}$  of OMNIImet•GUT solvent or EtOH 95%) to the tubes. We added 100  $\mu\text{L}$  of ultrapure water to make homogenization easier for samples with no preservative. All aliquots were homogenized with a bullet homogenizer (Next Advance) at a speed of 6 for 2 min. During sample processing, fast freezing of one aliquot per biological replicate was prioritized. Those aliquots were frozen within 15–20 min from defecation, and hereafter, this refers to the golden standard.

After the initial sample processing, the aliquots with no preservative (the crude sample), with OMNIImet•GUT solvent, and with EtOH 95% were stored at room temperature (RT) for 24, 36, 48 h, and 7 days. Additionally, the aliquots with EtOH 95% were kept at  $+4\text{ }^{\circ}\text{C}$  for 24, 36, 48, and 7 days. The crude samples were kept at  $+4$  for 24 h.

For the microbiome profiling, the sample material left from the spatula-mixed biological replicates were divided into aliquots of three sample types: feces with no preservative (crude feces), feces in EtOH 95%, and feces with OMNIgene.

GUT kit was in the same ratio as above. The aliquots of crude feces were frozen at  $-80\text{ }^{\circ}\text{C}$  within 2 h (kept on ice) from defecation. The aliquots with EtOH 95% and OMNIgene-GUT were stored at RT for 2 h, 48 h, and 7 days. After the incubation time, these aliquots were stored at  $-80\text{ }^{\circ}\text{C}$  until sample preparation for DNA extraction.

**Metabolite Extractions.** Here, three distinct extraction procedures were performed. Prior to extraction, we balanced the sample weights with liquid volumes by adding  $100\text{ }\mu\text{L}$  of water to EtOH/Omni-tubes and  $600\text{ }\mu\text{L}$  of EtOH to the crude samples and those labeled as “immediately frozen samples.”

First, we combined extraction for SCFA, bile acids (BAs), and untargeted metabolites assay. Glycoursodeoxycholic acid (GUDCA) -d4, glycocholic acid (GCA)-d4, cholic acid (CA) -d4, ursodeoxycholic acid (UDCA) -d4, glycochenodeoxycholic acid (GCDCA) -d4, chenodeoxycholic acid (CDCA) -d4, deoxycholic acid (DCA) -d4, glycolithocholic acid (GLCA) -d4, heptadecanoic acid, deuterium-labeled valine, deuterium-labeled succinic acid, deuterium-labeled glutamic acid, mass-labeled PFCAs and PFASs solution/mixture (MPFAC-MXA), and d4-androsterone were added as internal standards. After vortexing, samples were filtered through 96-well protein precipitation plates (Supelco/Sigma-Aldrich) with vacuum. Filtrates were divided into 3 parts ( $20\text{ }\mu\text{L}$  for BAs,  $20\text{ }\mu\text{L}$  for untargeted metabolites, and  $50\text{ }\mu\text{L}$  for SCFA). Vials for BA analysis were dried under nitrogen, resuspended in  $20\text{ }\mu\text{L}$  of methanol in water (4:6 v/v), and stored at  $-80\text{ }^{\circ}\text{C}$  until analysis. Vials for untargeted metabolites were dried and stored at  $-80\text{ }^{\circ}\text{C}$  before analysis. Filtrates for SCFA were stored in Waters deep well plates at  $-80\text{ }^{\circ}\text{C}$ .

The second extraction was for endocannabinoids (ECCs), and it included  $200\text{ }\mu\text{L}$  of fecal slurry and  $400\text{ }\mu\text{L}$  of crash solvent (95% Ethanol). To avoid contact with plastic, glass vials and syringes were utilized during extraction. Samples were vortexed and incubated for 30 min at  $-20\text{ }^{\circ}\text{C}$  and then filtered through the protein precipitation plate. The filtrates were evaporated under a gentle steam of nitrogen at  $+35\text{ }^{\circ}\text{C}$  and reconstituted with the final solvent  $50\text{ }\mu\text{L}/\text{sample}$  (40% water, 30% ACN, and 30% IPA) before the run. This crash solvent included the following internal standards: THC-COOH-d9, 2-AG-d5, NADA-d8, AEA-d8, and AA-d8.

The third extraction was for lipids done using liquid-liquid extraction, a method based on the Folch procedure, as described previously.<sup>19</sup> Here,  $10\text{ }\mu\text{L}$  of 0.9% NaCl and  $120\text{ }\mu\text{L}$  of crash solvent  $\text{CHCl}_3:\text{MeOH}$  (2:1, v/v) containing internal standards solution were added to  $10\text{ }\mu\text{L}$  of fecal sample homogenate. The crash solvent included the following internal standards: PE (17:0/17:0), SM(d18:1/17:0), Cer (d18:1/17:0), PC (17:0/17:0), LPC (17:0), PC (16:0/d31/18:1), and TG (17:0/17:0/17:0). After vortexing, samples were allowed to stand on ice for 30 min. Then, the samples were centrifuged ( $9400g$ , 5 min,  $4\text{ }^{\circ}\text{C}$ ). Next,  $60\text{ }\mu\text{L}$  of the lower layer was collected and transferred to an LC vial with an insert, and  $60\text{ }\mu\text{L}$  of  $\text{CHCl}_3:\text{EtOH}$  (2:1, v/v) was added. The extracts were stored at  $-80\text{ }^{\circ}\text{C}$  until analysis.

**Metabolite Analysis. Targeted Analysis.** Targeted methods were used for SCFA, BAs, and ECCs.

**Bile Acid Analysis.** For BA analysis, the chromatographic separation was carried out using an Acquity Premiere HSS T3 column ( $100\text{ mm} \times 2.1\text{ mm i.d.}$ ,  $1.8\text{ }\mu\text{m}$  particle size), fitted with a C18 precolumn (Acquity UPLC HSS T3  $1.8\text{ }\mu\text{m}$ ,  $2.1\text{ mm} \times 5\text{ mm}$ , Waters Corporation, Wexford, Ireland). Mobile phase A consisted of water:methanol (v/v 70:30), and mobile

phase B consisted of methanol, with both phases containing 2 mM ammonium acetate as an ionization agent. The flow rate was set at  $0.4\text{ mL}/\text{min}$ , with the elution gradient as follows: 0–1.5 min, mobile phase B was increased from 5 to 30%; 1.5–4.5 min, mobile phase B was increased to 70%; and 4.5–7.5 min, mobile phase B was increased to 100% and held for 5.5 min. A post-time of 5 min was used to regain the initial conditions for the next analysis. The total run time per sample was 18 min. The injection volume used was  $5\text{ }\mu\text{L}$ . The analyses were performed in negative ion mode, and Analyst v. 1.7.3 (AB SCIEX) was used for all data acquisition. For other details of the method, see the Supporting Information method M1.

**SCFA Analysis.** For SCFAs, the sample aliquot was derivatized by adding  $50\text{ }\mu\text{L}$  of 50 mM 3-nitrophenylhydrazine (3-NPH) in 3:7 H<sub>2</sub>O: MeOH, followed by addition of  $50\text{ }\mu\text{L}$  of 50 mM ethylene dichloride (EDC) in 3:7 H<sub>2</sub>O: MeOH,  $50\text{ }\mu\text{L}$  of pyridine (7% v/v in 3:7 H<sub>2</sub>O: MeOH). The mixture was then incubated for 60 min at room temperature, after which  $100\text{ }\mu\text{L}$  of formic acid (0.2% in 3:7 H<sub>2</sub>O: MeOH) was added to the mixture to quench the reaction. The analysis of derivatized SCFAs was carried out on an Acquity UPLC BEH C18 column ( $2.1\text{ mm} \times 100\text{ mm}$ ,  $1.7\text{ }\mu\text{m}$ ; Waters, Milford) using as mobile phase (A) 0.1% formic acid in water and (B) 0.1% formic acid in acetonitrile. Samples were eluted at  $0.5\text{ mL min}^{-1}$ , starting with 10% B and increasing to 100% B in 10 min, then holding at 100% B for 2.1 min, returning to 10% B and holding for 2 min. Column temperature was maintained at  $50\text{ }^{\circ}\text{C}$ , while the autosampler was maintained at  $10\text{ }^{\circ}\text{C}$  during analysis. The injection volume was  $5\text{ }\mu\text{L}$ . The analyses were performed in negative ion mode, and Analyst v. 1.7.3 (AB SCIEX) was used for all data acquisition. For other details of the method, see Supporting Information method M2.

**Endocannabinoid Analysis.** The ECCs analysis was carried out on an XBridge BEH C18 column ( $2.1\text{ mm} \times 150\text{ mm}$ ,  $2.5\text{ }\mu\text{m}$ ; Waters, Milford) using as mobile phase (A) 1 mM ammonium acetate and 0.1% formic acid in water and (B) 1 mM ammonium acetate and 0.1% formic acid in ACN: IPA (1:1). Samples were eluted at  $0.4\text{ mL}/\text{min}$ , starting with 60% B and holding for 0.3 min, then increasing to 100% for 5 min, holding at 100% B for 2.5 min, returning to 10% in 0.1 min, and holding for 3 min. Column temperature was maintained at  $40\text{ }^{\circ}\text{C}$ , while the autosampler was maintained at  $15\text{ }^{\circ}\text{C}$  during analysis. The injection volume was  $10\text{ }\mu\text{L}$ . The analyses were performed in positive and negative ion mode, and SCIEX OS v3.0 (AB SCIEX) was used for all data acquisition. For other details of the method, see Supporting Information method M3 and related publications.<sup>19</sup>

SCFAs and BAs were analyzed with an Exion LC system coupled to a QTrap 5500 MS interfaced with a Turbo V electrospray ion source (SCIEX, Framingham, MA). The ECCs were analyzed with an Exion LC system coupled with a QTrap 7500 MS interfaced with an OptiFlow Pro electrospray ion source (SCIEX, Framingham, MA). The lipids were analyzed with an Exion LC system coupled with TripleTOF 6600 MS interfaced with a DuoSpray electrospray ion source (SCIEX, Framingham, MA).

**Untargeted Analysis.** Lipids and polar metabolites were analyzed using a combination of untargeted and semitargeted assays. Lipids were quantified using class-based internal standards and authentic standards from each class. Polar metabolites were quantified using a set of internal standards, as described below.

**Lipidomic Analysis.** The lipidomic analysis was carried out on an ACQUITY UPLC BEH C18 column (2.1 mm × 100 mm, particle size of 1.7 μm) by Waters (Milford). The eluent system consisted of (A) 10 mM ammonium acetate in H<sub>2</sub>O and 0.1% formic acid and (B) 10 mM ammonium acetate in ACN: IPA (1:1) and 0.1% formic acid. The gradient was as follows: an increase from 35% B to 80% B over 2 min and then an increase to 100% B over 5 min. The gradient was held at 100% B for 7 min, followed by a re-equilibration at 35% over 7 min. The injection volume was 1 μL. The column compartment and autosampler temperatures were 40 and 10 °C, respectively. All analyses were performed in positive ion mode, and Analyst v1.8.1 (AB SCIEX) was used for all data acquisition. The RSD% for QC samples (*n* = 8) was, on average, 18.95%.

Data was processed using MZmine 2.<sup>20</sup> Mass spectrometry data processing was performed using the open source software package MZmine 2.53.<sup>20</sup> The following steps were applied in this processing: (i) mass detection with a noise level of 1000, (ii) chromatogram builder with a minimum time span of 0.08 min, minimum height of 1000 and a *m/z* tolerance of 0.006 *m/z* or 10.0 ppm, (iii) chromatogram deconvolution using the local minimum search algorithm with a 70% chromatographic threshold, 0.05 min minimum RT range, 5% minimum relative height, 1200 minimum absolute height, a minimum ration of peak top/edge of 1.2, and a peak duration range of 0.08–5.0, (iv), isotopic peak grouper with a *m/z* tolerance of 5.0 ppm, RT tolerance of 0.05 min, maximum charge of 2 and with the most intense isotope set as the representative isotope, (v) Join aligner with a *m/z* tolerance of 0.009 or 10.0 ppm and a weight for of 2, a RT tolerance of 0.15 min and a weight of 1 and with no requirement of charge state or ID and no comparison of isotope pattern, (vi) peak list row filter with a minimum of 10% of the samples, (vii) gap filling using the same RT and *m/z* range gap filler algorithm with an *m/z* tolerance of 0.009 *m/z* or 11.0 ppm, and (viii) identification of lipids using a custom database search with an *m/z* tolerance of 0.008 *m/z* or 8.0 ppm and a RT tolerance of 0.25 min. Identification of lipids was based on in-house data on the LC-MS/MS retention time and mass spectra. The identification was done with a custom database, with identification levels 1 and 2, i.e., based on authentic standard compounds (level 1) and based on MS/MS identification (level 2) based on Metabolomics Standards Initiative.

Quantification of lipids was performed using a 7-point internal calibration curve (0.1–5 μg/mL) using the following lipid-class specific authentic standards: using 1-hexadecyl-2-(9*Z*-octadecenyl)-*sn*-glycero-3-phosphocholine (PC(16:0e/18:1(9*Z*))), 1-(1*Z*-octadecenyl)-2-(9*Z*-octadecenyl)-*sn*-glycero-3-phosphocholine (PC(18:0p/18:1(9*Z*))), 1-stearoyl-2-hydroxy-*sn*-glycero-3-phosphocholine (LPC(18:0)), 1-oleoyl-2-hydroxy-*sn*-glycero-3-phosphocholine (LPC(18:1)), 1-palmitoyl-2-oleoyl-*sn*-glycero-3-phosphoethanolamine (PE(16:0/18:1)), 1-(1*Z*-octadecenyl)-2-docosahexaenyl-*sn*-glycero-3-phosphocholine (PC(18:0p/22:6)) and 1-stearoyl-2-linoleoyl-*sn*-glycerol (DG(18:0/18:2)), 1-(9*Z*-octadecenyl)-*sn*-glycero-3-phosphoethanolamine (LPE(18:1)), N-(9*Z*-octadecenyl)-sphinganine (Cer(d18:0/18:1(9*Z*))), 1-hexadecyl-2-(9*Z*-octadecenyl)-*sn*-glycero-3-phosphoethanolamine (PE(16:0/18:1)) from Avanti Polar Lipids, 1-Palmitoyl-2-Hydroxy-*sn*-Glycero-3-Phosphatidylcholine (LPC(16:0)), 1,2,3 trihexadecanoalglycerol (TG(16:0/16:0/16:0)), 1,2,3-trioctadecanoylglycerol (TG(18:0/18:0/18:0)) and 3β-hydroxy-5-cholestene-

3-stearate (ChoE(18:0)), 3β-Hydroxy-5-cholestene-3-linoleate (ChoE(18:2)) from Larodan, were prepared to the following concentration levels: 100, 500, 1000, 1500, 2000, and 2500 ng/mL (in CHCl<sub>3</sub>:MeOH, 2:1, v/v), including 1250 ng/mL of each internal standard.

**Polar Metabolite Analysis.** For polar metabolites, aliquots of 10 μL of samples were injected into the Acquity UPLC BEH C18 2.1 mm × 100 mm, 1.7-μm column (Waters Corporation), fitted with a C18 precolumn (Waters Corporation, Wexford, Ireland). The mobile phases consisted of (A) 2 mM NH<sub>4</sub>Ac in H<sub>2</sub>O: MeOH (7:3) and (B) 2 mM NH<sub>4</sub>Ac in MeOH. The flow rate was set at 0.4 mL min<sup>-1</sup> with the elution gradient as follows: 0–1.5 min, mobile phase B was increased from 5 to 30%; 1.5–4.5 min, mobile phase B was increased to 70%; 4.5–7.5 min, mobile phase B was increased to 100% and held for 5.5 min. A post-time of 5 min was used to regain the initial conditions for the next analysis. The total run time per sample was 20 min. The dual ESI ionization source settings were as follows: capillary voltage was 4.5 kV, nozzle voltage was 1500 V, N<sub>2</sub> pressure in the nebulizer was 21 psi, and the N<sub>2</sub> flow rate and temperature as sheath gas were 11 Lmin<sup>-1</sup> and 379 °C, respectively. In order to obtain accurate mass spectra in the MS scan, the *m/z* range was set to 100–1700 in negative ion mode. MassHunter B.06.01 software (Agilent Technologies, Santa Clara, CA) was used for all data acquisition. The RSD% for QC samples (*n* = 8) was, on average, 18.76%.

Quantitation was done using 6-point calibration (bile acids, ca. 20–640 ng/mL; polar metabolites, ca. 0.1 to 80 μg/mL). Quantification was performed using the following compounds: chenodeoxycholic acid (CDCA), cholic acid (CA), deoxycholic acid (DCA), glycochenodeoxycholic acid (GCDCA), glycocholic acid (GCA), glycodehydrocholic acid (GDCA), glycodeoxycholic acid (GDCA), glychoyocholic acid (GHCA), glycohyodeoxycholic acid (GHDCA), glycolitocholic acid (GLCA), glycoursodeoxycholic acid (GUDCA), hyocholic acid (HCA), hyodeoxycholic acid (HDCA), lithocholic acid (LCA), α-Muricholic acid (αMCA), tauro-α-muricholic acid (T-α-MCA), tauro-β-muricholic acid (T-β-MCA), taurochenodeoxycholic acid (TCDCA), taurocholic acid (TCA), taurodehydrocholic acid (THCA), taurodeoxycholic acid (TDCA), taurohyodeoxycholic acid (THDCA), taurolithocholic acid (TLCA), tauro-omega-muricholic acid (TωMCA) and tauroursodeoxycholic acid (TDCA), alanine, citric acid, fumaric acid, glutamic acid, glycine, lactic acid, malic acid, 2-hydroxybutyric acid, 3-hydroxybutyric acid, linoleic acid, oleic acid, palmitic acid, stearic acid, cholesterol, fructose, glutamine, indole-3-propionic acid, isoleucine, leucine, proline, succinic acid, valine, asparagine, aspartic acid, arachidonic acid, glycerol-3-phosphate, lysine, methionine, ornithine, phenylalanine, serine, and threonine.

Quality control was accomplished both for lipidomics and for polar metabolites by including blanks, pure standard samples, extracted standard samples, pooled quality control samples, and control plasma samples. The pooled samples were prepared by taking an aliquot (10 μL) of each extract separately for lipidomic and polar metabolite methods, and pooling them and aliquoting the pool into separate vials. In lipidomic and metabolomic analyses, lipids and metabolites that had >30% RSD in the pooled QC samples (an equal aliquot of each sample pooled together) or that were present at high concentrations in the extracted blank samples (ratio

between samples to blanks <5) were excluded from the data analyses.

**Gut Microbiome Analysis.** For microbiome profiling, the same fecal samples as above ( $n = 4$ ) were tested (including 3 biological replicates) with three sample collection types: immediately frozen crude feces, feces in EtOH 95%, and OMNIgene. GUT kit in ratio 1:4 (150 mg +600  $\mu$ L); samples in 95% EtOH and OMNIgene. GUT were kept at RT for 24, 48, and 7 days and then stored at  $-80$  °C until DNA extraction. The sample volume was 50 mg per DNA extraction, either as crude or dissolved in a preservative. Microbial DNA was extracted using a DNA Stool 200 Kit special H96 (PerkinElmer, Turku, Finland) kit with a corresponding Chemagic with Magnetic Separation Module I (MSM I) extraction robot after bead-beating and proteinase K incubation. Microbial composition was determined by sequencing the V3 V4 region of the 16S ribosomal gene using a MiSeq platform (Illumina). The sequence library was constructed according to the Illumina library preparation protocol, with minor differences from the V3 V4 protocol. After PCR, 8  $\mu$ L of the integrity of the product was analyzed with 1.5% TAE agarose gel (120 V, 1 h). The concentration of the library samples was measured with a Qubit Fluorometer by using a Qubit dsDNA High Sensitivity Assay kit. The 4 nM library pool was denatured and diluted to a concentration of 4pM, and an 8% denaturalized PhiX control (Illumina) was added. The library samples were sequenced with a MiSeq Reagent kit v3, 600 cycles (Illumina) on a Miseq system with 2 $\times$  300 base pair (bp) paired ends following the manufacturer's instructions. A positive control, Zymobiomics Microbial community DNA standard (Zymo Research), and a negative control (PCR-grade water) were included in library preparation to control the PCR. Lysis buffer was used as the negative control in DNA extraction to control contamination.

**Statistical Analysis.** For metabolomics data, all multivariate statistical analyses were based on log<sub>2</sub>-transformed intensity data. The transformed data were auto-scaled prior to multivariate analysis to improve the global interpretability. To account for the inconsistency in the fecal water content, the measured metabolites were normalized to the dry weight in the stool. The multivariate analysis was done using the PLS Toolbox 8.2.1 (eigenvektor Research Inc., Manson, WA) in MATLAB 2017b (Mathworks, Inc., Natick, MA). ANOVA-simultaneous component analysis (ASCA), a multivariate extension of ANOVA analysis, was performed to allow interpretation of the variation induced by the different factors, including time, individual, and collection matrix. Subsequently, for univariate analysis, the level of each metabolite in each sample storage matrix (i.e., crude feces without any solvent, feces in 95% EtOH, and feces in OMNIgene•GUT) was divided by the level of the same metabolite species in the paired immediately frozen sample (golden standard sample). For instance, the concentration of butyrate in the 95% EtOH was divided by the concentration of butyrate in the immediately frozen sample (golden standard). The fold difference was calculated by dividing the mean concentration of a given metabolite species in one group by another. The difference in the metabolites between the groups was tested using a multivariate linear model using the MaAsLin2 package in R, taking into account random effects within an individual sample or subject. The resulting nominal p-values were corrected for multiple comparisons using the Benjamini and Hochberg approach. The adjusted p-values <0.25 (q-values)

were considered significantly different among the group of hypotheses tested.

Microbiome data analyses were performed in R Bioconductor ecosystem (R version 4.2.3) and with a CLC Microbial Genomics Module (CLC Genomics Workbench 21.0.3, Qiagen), which complies with QIIME2.<sup>21</sup> Differences in  $\beta$  diversity between methodological settings were evaluated with distance-based redundancy analysis and PERMANOVA. We used the Bray–Curtis dissimilarity. Moreover,  $\beta$  diversity by Jaccard, UniFrac, and Unweighted UniFrac were plotted. We calculated the Shannon index, number of observed OTUs and Chao1, and the Simpson Index. All of the indices were used in the ICC testing. Differences in the Shannon index were assessed with two sample *t* tests assuming equal variance (Levene's test).

## RESULTS AND DISCUSSION

**Fecal Metabolome and Lipidome Profiles.** Fecal metabolites and lipids were analyzed from a total of 168 fecal samples (aliquoted from four individuals) simulating different conditions of the sample storage matrix: (i) crude feces without any solvent, (ii) feces in 95% EtOH, and (iii) feces in OMNIgene•GUT solvent. For each sampling condition, we obtained samples from three different parts of the bulk fecal specimen (Figure 1, Part 1–3). To investigate the effects of storage time and temperature, initially, we obtained one aliquot of the homogenized fecal sample and froze it immediately at  $-80$  °C, which was used as a reference (golden standard) sample (Figure 1). Other corresponding aliquots were tested for varying durations at different temperatures: 24 h at +4 °C (except OMNIgene•GUT), 24 h at room temperature (RT), 36 h at RT, 48 h at RT, 48 h at +4 °C (except OMNIgene•GUT), and 7 days at RT, as shown in Figure 1.

The metabolomics analysis included targeted short-chain fatty acids (SCFA,  $n = 7$ ) and bile acids (BAs,  $n = 33$ ), encompassing both primary (glycine/taurine conjugates) and secondary BAs, as well as endocannabinoids (ECCs,  $n = 9$ ). These ECCs included palmitoylethanolamide (PEA), arachidonoylglycerol (AG), 2-arachidonoylglycerol ether (2-AGE), arachidonylethanolamide (AEA), oleoylethanolamide (OEA), stearoylethanolamide (SEA), docosahexaenoylethanolamide (DEA),  $\alpha$ -linolenoyl ethanolamide (aLEA), and arachidonic acid (AA). Lipidomics analysis provided coverage of the following lipid classes: acylcarnitines (AC), cholesterol esters (CE), ceramides (Cer), diacylglycerols (DG), lysophosphatidylcholines (LPC), phosphatidylcholines (PC), sphingomyelins (SM), and triacylglycerols (TG). Untargeted polar metabolomics analysis provided coverage of the following classes: amino acids, bile acids, carboxylic acids (mainly free fatty acids and other organic acids), hydroxy acids, phenolic compounds, alcohols, and sugar derivatives.

**Fecal Metabolic Profile. Multifactorial Analysis.** To understand the contributions of different sampling factors to the fecal metabolome, we performed analysis of variance (ANOVA)-simultaneous component analysis (ASCA) with the following factors: subjects; sample storage matrix (crude, 95% EtOH, OMNIgene•GUT, immediately frozen); time (24, 36, 48 h, 7 days); and temperature (RT, +4 °C). ASCA is a multivariate extension of ANOVA analysis that allows interpretation of the variation induced by the different factors, including individual, sample storage, and time. We found that interindividual differences (Model Effect (%)) 71.15, 65.10,

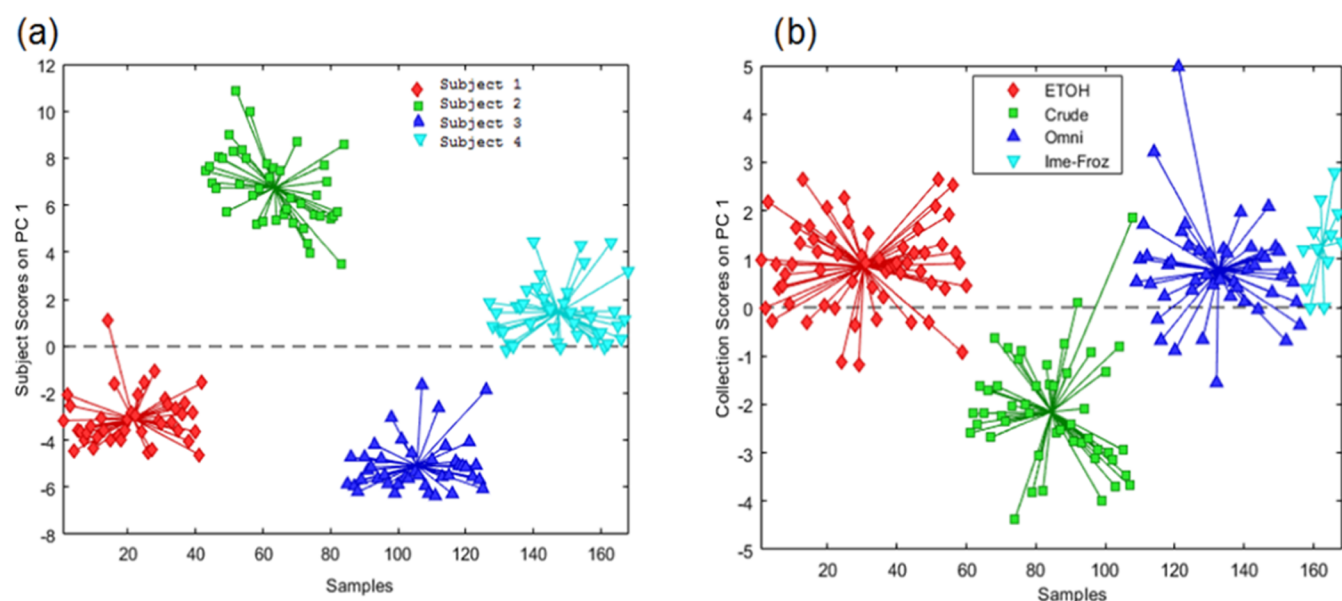


**Figure 2.** Principal component analysis (PCA) score plots based on ANOVA-simultaneous component analysis (ASCA). (a) Principal component (PC1) score plot obtained based on interindividual score in ASCA analysis. This figure represents the bile acid data set arranged according to interindividual samples in the PCA score plot. Here, each sample is represented by a point and colored according to the individual (red diamond: Subject1, green square: Subject 2, blue triangle up: Subject 3, cyan triangle down: Subject4). (b) Principal component (PC1) score plot obtained based on sample storage matrix score in ASCA analysis. This figure represents the bile acid profile arranged according to the sample storage matrix in the PCA score plot. Here, each sample is represented by a point and colored according to the sample storage matrix (red diamond: 95% EtOH, green square: crude, blue triangle up: OMNImet•GUT, cyan triangle down: immediately frozen).

77.70,  $p = 0.0010$ ) and subsequent sample storage matrix (Model Effect (%) 8.2, 9.6, 2.5,  $p = 0.0010$ ) had the strongest effect on BAs, SCFAs, and ECCs fecal profiles. In comparison, the ASCA could not find significant effects of the duration of storage (Model Effect (%) 2.1, 2.0, 1.7,  $p > 0.05$ ) and storage temperature (Model Effect (%) 1.60, 1.09, 1.34,  $p > 0.05$ ). Figure 2 illustrates the clustering differences in the subject (Figure 2a) and sample storage matrix (Figure 2b) explained by the levels of fecal BAs. Similar trends were observed for SCFAs and ECCs (Supporting Information Figures S1 and S2). Similar analysis utilizing untargeted lipidomics and polar metabolites (see Supporting Information Figure S3) found only a minor intersubject significant effect (Model Effect (%) 15.3, 19.9,  $p = 0.0010$ ), with no contribution of the sample storage matrix, storage time, and temperature ( $p > 0.05$ ). This may be attributed to larger within-group variance.

**Metabolic Changes throughout Storage at Room Temperature.** To better understand the effects of sample storage duration (24, 36, 48 h, 7 days) at room temperature on the fecal metabolome, we analyzed the stability of metabolites in aliquots stored without solvent (crude), with 95% EtOH, and with an OMNImet•GUT tube. For each sample matrix, we calculated the relative change of each metabolite compared with the gold standard (immediately frozen sample).

We found that SCFAs in the crude samples increased over time, while a stable profile was recorded in sample aliquots stored in a 95% EtOH or OMNImet•GUT tube. In particular, butyric acid, isobutyric acid, and valeric acid increased over 1.5 fold in raw feces left at RT from 24 h until 48 h (Figure 3a,b,  $p_{\text{adj}} < 0.25$ , Supporting Information Figure S4 and Table S1), suggesting continuous microbial activity over time. We also observed an increase in the levels of butyric acid, isobutyric acid, and valeric acid by 1.72, 1.73, and 1.47-fold (FC), respectively, within the first 24 h compared to the sample that

was frozen immediately. However, we observed a stable pattern of these SCFAs in fecal samples collected with 95% EtOH and/or OMNImet GUT solvent (Figure 3 and Supporting Information Figure S4 and Tables S2–S3). Taken together, crude feces (stored without any solvent) at room temperature showed at least a 50% increase in SCFA over 24–48 h. SCFAs are primarily produced by gut microbes through the saccharolytic fermentation of complex microbiota-accessible carbohydrates (MACs).<sup>22,23</sup> Therefore, our results suggest that crude samples at room temperature are susceptible to microbial metabolism by specific microorganisms encoding MAC-degrading enzymes. This is corroborated by the increased SCFA levels we recorded at room temperature when compared to samples stored at 4 °C. These results suggest that 95% EtOH can inhibit microbial activity such as saccharolytic fermentation even at room temperature, which, in turn, can prevent and reduce metabolite degradation. However, there were exceptions of conjugated BAs such as GLCA, GCDCA, GDCA, GCA, and several unknown metabolites (Supporting Information Tables S4–S5) that appeared to be affected by temperature (nominal  $p$ -value  $< 0.05$ ) and require further investigation.

No consistent time-dependent pattern was found during 7 days of storage at room temperature in all sample storage matrices (crude, 95% EtOH, OMNImet•GUT, immediately frozen), with the exception of SCFA in crude feces. We also analyzed the concentration differences of fecal BAs, lipids, and metabolites over time in these sampling groups. Tauro- and/or glycoconjugated bile acids (GLCA, THDCA, GCDCA), lipids (mainly TGs), and unknown polar features increased over time ( $p < 0.05$ ) and differed in at least one of the three sample storage matrices. However, none of these metabolites exceeded the significance level at the selected FDR threshold of 0.25 (Figure 3c,d, Supporting Information Figures S5–S7, and

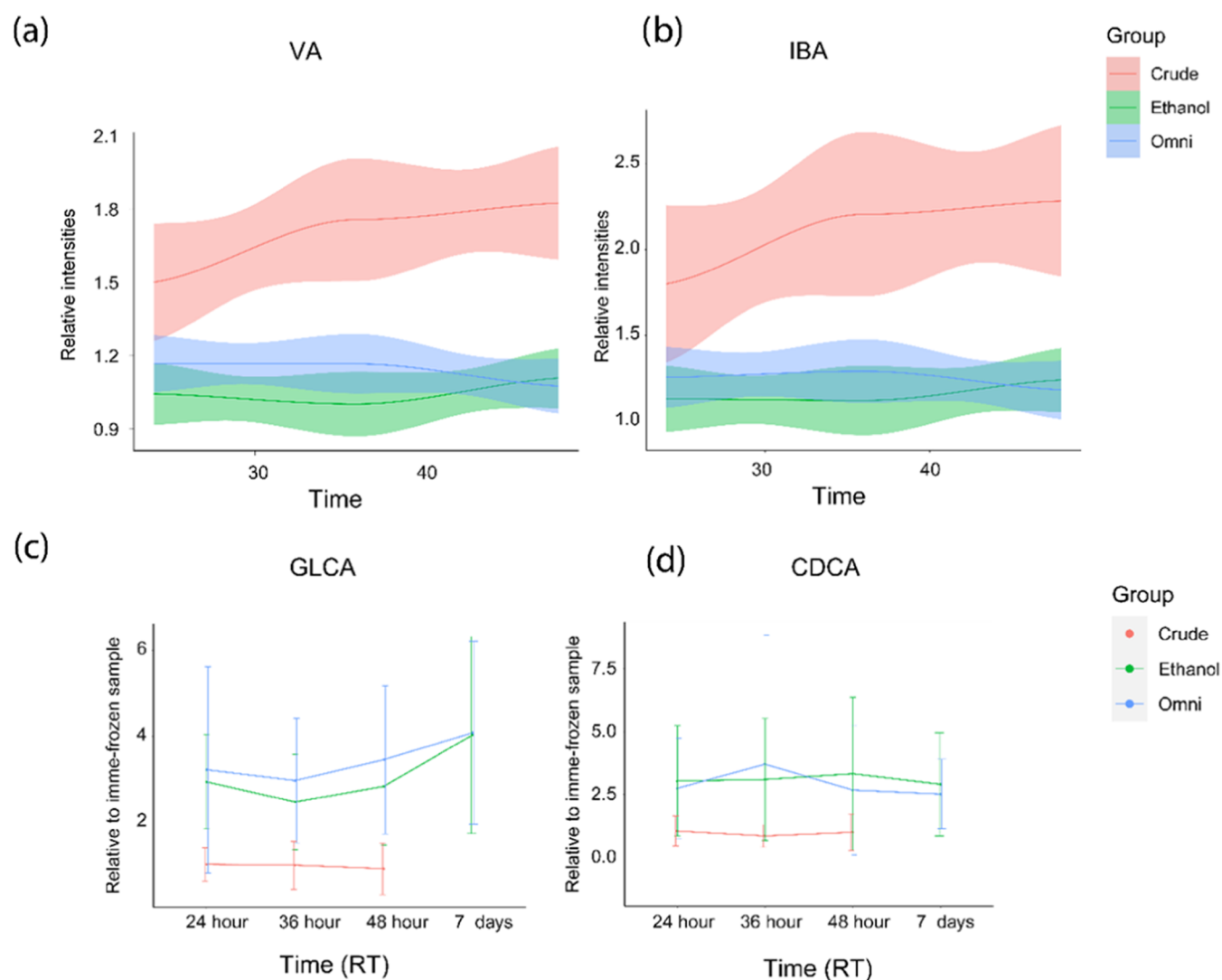


**Figure 3.** Alterations in metabolites during storage at room temperature. A Loess curve plot showing the changes in the levels of two SCFA [(a) Valeric acid and (b) Isobutyric acid] over time (24, 36, 48 h) in feces samples collected as crude, in 95% EtOH, and with OMNImet•GUT solvent. The X-axis shows the sample storage duration (24, 36, and 48 h). The Y-axis shows the relative change of each metabolite compared to the gold standard. VA is valeric acid, and IBA is isobutyric acid. The changes in bile acids (BAs) over time (24, 36, 48, and 7 days) were examined in feces samples collected in three different ways: crude, in 95% EtOH, and in OMNImet•GUT solvent. (c) Glycolithocholic acid (GLCA) and (d) Chenodeoxycholic acid (CDCA).

Tables S1–S3). Research investigating the gut microbiome–metabolome relationship has predominantly concentrated on water-soluble polar metabolites, with microbe-linked lipids receiving less emphasis.<sup>24–26</sup> To aid in this effort, apart from the methodological comparison, our results also highlight that fecal lipids can serve as a functional indicator of gut microbial metabolism.

**Fecal Metabolic Changes in 95% Ethanol at Different Temperatures.** We compared the differences of individual metabolite levels between fecal aliquots stored at room temperature and at +4 °C in a 24 h sample set. We found significant changes in microbial metabolites, including conjugated bile acids and SCFAs. GLCA content was 1.31 FC higher in samples stored at room temperature than in fecal aliquots stored at +4 °C in 95% EtOH (Figure 4). In crude feces, two BAs [7-oxo DCA (FC = 4.1), DHCA (FC = 0.45)] and five SCFAs, including acetic acid (FC = 1.51), butyric acid (FC = 1.64), isobutyric acid (FC = 1.37), valeric acid (FC = 1.28), propionic acid (FC = 1.32), and the internal stability

standard Butyric acid-<sup>13</sup>C<sub>4</sub> (FC = 0.51) changed when stored at RT (Figure 4, Supporting Information Tables S4–S5). In contrast, the corresponding metabolites (e.g., SCFAs) remained stable in fecal samples collected in 95% EtOH, which may be partly due to active enzymatic metabolism by the gut microbiota at room temperature but not when deactivated by 95% EtOH (Supporting Information Tables S4–S5).

We generally observed good metabolite stability in the 95% EtOH and OMNImet•GUT kits, irrespective of the storage temperature. Our findings are consistent with previous studies suggesting that fecal samples in 95% EtOH or OMNImet•GUT have comparable metabolite profiles to samples that were frozen shortly after collection.<sup>10,13,15,27</sup> In addition, 95% EtOH was reported to be the most suitable matrix for preserving the fecal metabolite profile in comparison to clinically used fecal collection kits that do not target metabolites (RNAlater, OMNIgene•GUT, fecal occult blood test (FOBT) cards).<sup>15,27</sup> Feces collected without any solvent was suitable for

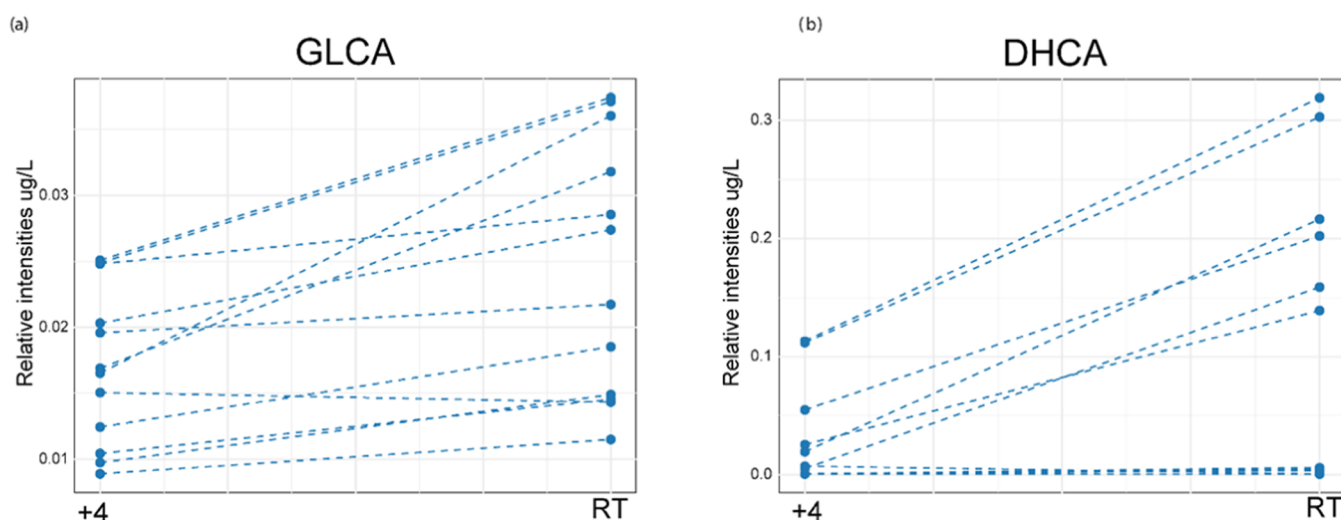


**Figure 4.** Stability of fecal metabolites at room temperature (RT) compared to +4 °C for (a) 95% EtOH samples and (b) crude samples. The Y-axis denotes concentration of metabolites, and the X-axis denotes the different temperatures (+4 °C and RT). GLCA is glycolithocholic acid, and DHCA is dehydrocholic acid.

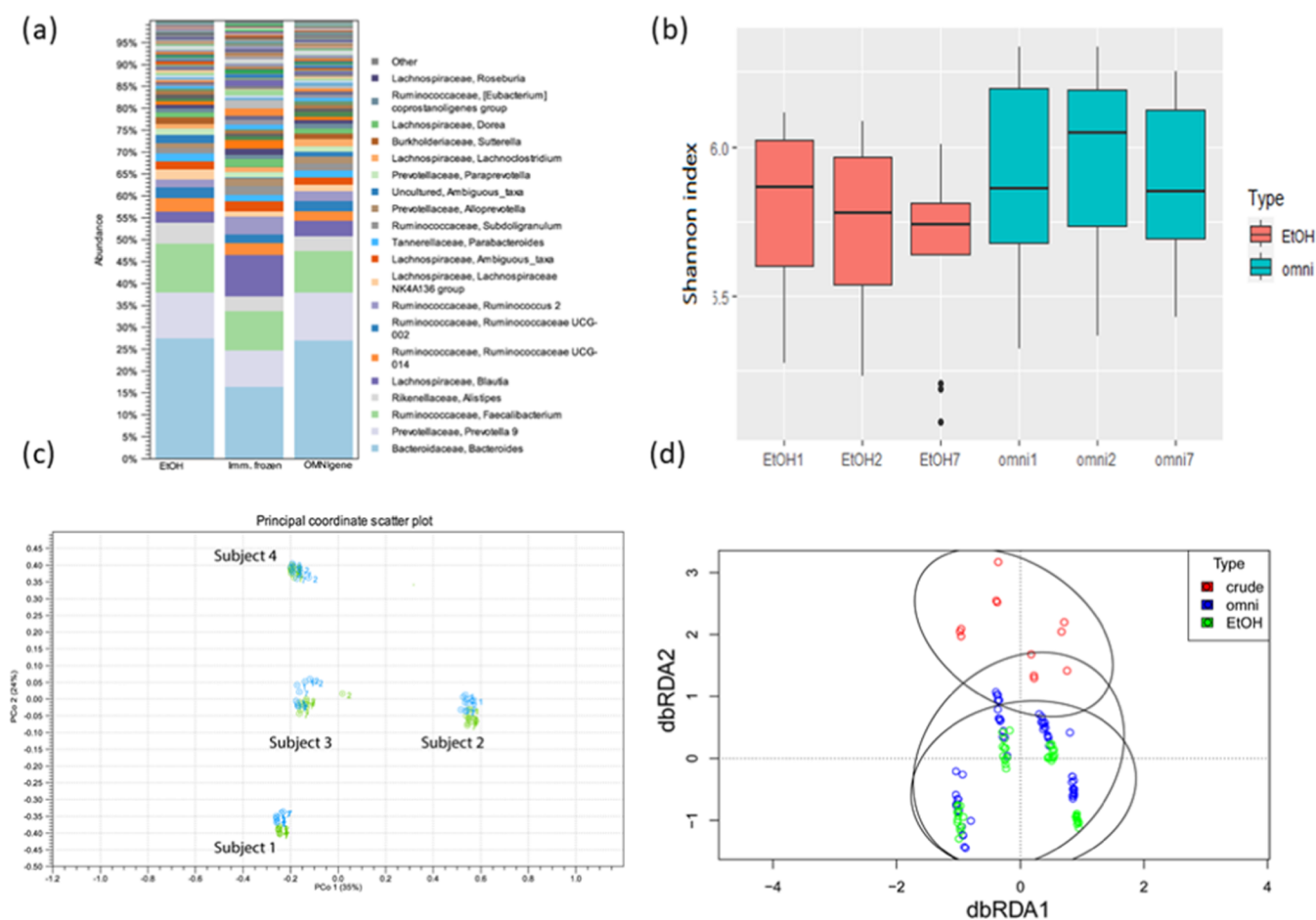


**Figure 5.** Stability of the fecal microbiome in 95% EtOH stored at RT. (a) Microbiome profiles by relative abundances in different storage types. Legend shows 20 most abundant genera. Main genera are the same; abundances differ between immediately frozen samples and samples in preservatives. (b)  $\alpha$  diversity (Shannon index) by storage type and time. Numbers indicate days of storage. (c)  $\beta$  diversity by Principal Coordinates analysis with Bray–Curtis dissimilarity metrics. Colors indicate storage types with the number of storage days. Green and blue circles represent 95% EtOH and OMNIgene•GUT, respectively. (d) Distance-based redundancy analysis with Bray–Curtis representing dissimilarity between storage types with ellipses of 95% confidence interval.

metabolomics analysis when frozen immediately after collection.<sup>15</sup> However, it is worth noting that this approach

is inconvenient, expensive, and not feasible for population-based studies on a large scale. Liu et al. demonstrated that

metabolite measures obtained from OMNIgene•GUT were comparable to those obtained from samples that were immediately frozen after collection for up to 21 days. These findings suggest that OMNIgene•GUT is sufficient for obtaining data on the gut microbiome and gut metabolome.<sup>14</sup> On the contrary, other studies report that OMNIgene•GUT may not be optimal for collecting fecal samples for metabolomics profiles.<sup>10,27</sup>

To our knowledge, this is the first study to directly compare the performance of the OMNImet•GUT kit, which is designed to preserve fecal metabolites at room temperature, to flash freezing feces or using 95% ethanol. Unlike similar studies, we also utilized internal standards and biological replicates to assess the stability of the detected metabolites at room temperature. We applied a wide range of metabolomics platforms: targeted metabolomics to measure SCFA, BAs, and endocannabinoids, as well as untargeted metabolomics to detect lipids and polar metabolites. Various studies have shown that both the human gut microbiota and metabolome are highly heterogeneous between individuals.<sup>28–30</sup> Indeed, our work showed that variance between fecal samples was mainly attributed to interindividual differences and affected by the sample storage matrix, while less affected by the duration at room temperature when stored in 95% EtOH and OMNImet•GUT liquid. This is consistent with similar work, where metabolite concentrations have been shown to vary considerably between individuals.<sup>31,32</sup> Besides that, we also found that the metabolome pattern varied across different parts of the fecal specimen (Supporting Information Figure S8). This is in line with previous studies suggesting that metabolites may not be evenly distributed within the fecal samples.<sup>31,33</sup> Trost et al. studied the variation in metabolites from four sampling areas of cryogenically collected fecal specimens and found that fecal metabolites are not homogeneously distributed within the specimens.<sup>32</sup> Similarly, Jones et al. also showed that SCFA concentrations vary profoundly across a single stool.<sup>31</sup> Pooling of the samples from different parts of the stool could be considered to minimize variation arising from the sampling.<sup>32,34</sup>

**Fecal Microbiome Profile.** We aimed to determine the stability of the fecal microbiome in 95% EtOH stored at RT. The composition of the fecal microbiota was analyzed by 16S rRNA gene sequencing using the V3–V4 hypervariable region ( $n = 118$ ). These samples correspond to aliquots obtained from the fecal sample that were frozen straight after processing at  $-80\text{ }^{\circ}\text{C}$  while other aliquots were stored for 24 h, 48 h, and 7 days at RT in 95% EtOH and OMNIgene•GUT (Figure 1). The bacterial profiles with relative abundances from these collections are shown in Figure 5a and are summarized for all subjects and time points. We found that the bacterial profiles of the fecal samples stored in 95% EtOH and OMNIgene•GUT were similar. However, the immediately frozen samples differed from those stored in 95% EtOH and OMNIgene•GUT, mainly by *Bacteroides* and *Blautia*. Positive controls included in the NGS-protocol indicated high reproducibility, and the accuracy was sufficient based on the theoretical and identified abundances (Supporting Information Figure S9).

Similarly, we analyzed the differences in the  $\alpha$  diversity among the three study groups. We found that interindividual differences had a dominant effect on microbiome  $\alpha$  diversity (Supporting Information Figure S10). Lower  $\alpha$  diversity was observed in both storage solvents compared with immediately frozen samples. We also found a significant decrease in the  $\alpha$

diversity in the longitudinal series of samples collected in 95% EtOH. Figure 5b shows that  $\alpha$  diversity was lower over time in 95% EtOH compared with OMNIgene•GUT ( $p = 0.007$ ). We also compared similarities between storage types using intraclass correlation coefficients with immediately frozen samples used as reference (ICC, see Supporting Information Figure S11). We compared similarity in  $\alpha$  diversity metrics (Shannon, Simpson, Chao1, number of observed OTUs) and three most prevalent genera (*Bacteroides*, *Bifidobacterium*, and *Faecalibacterium*) between storage types. OMNIgene•GUT showed higher  $\alpha$  diversity intraclass similarity with the immediately frozen samples than in the 95% EtOH samples.

Additionally, we also analyzed the differences in overall gut microbiota composition, i.e.,  $\beta$  diversity between samples collected in 95% EtOH and OMNIgene•GUT. PcoA with Bray–Curtis dissimilarity showed little difference between storage types and time points (Figure 5c). PcoA with Jaccard, UniFrac, and Unweighted UniFrac showed parallel results; however, there were fewer differences with UniFrac metrics (Supporting Information Figures S12–S13). However, the score plot revealed that interindividual variability is the key factor shaping the fecal microbiome (Figure 5d). There were no significant differences in  $\beta$  diversity between storage types (distance-based redundancy analysis with Bray–Curtis dissimilarity, PERMANOVA,  $p = 0.3$ ). However, interindividual differences were significant ( $p = 0.001$ ), as expected. Meanwhile, the variation among biological replicates of a single individual was low (Figure S14).

**Limitations.** We acknowledge that there are some limitations that must be considered. The main limitation is that instead of collecting directly within each inspected matrix, we only simulated such collection; however, samples were processed immediately. This is an inherent technical limitation of the study design, which requires aliquots of the same biological sample to be compared across various collection matrices and storage conditions. Our study suggests that the metabolomes of different portions of whole feces vary profoundly. We acknowledge that aliquots of feces may not represent the entire specimen accurately. However, pooled sampling across the whole specimen may be a strategy to account for the intrasample variance. Additionally, we recognize a discrepancy in the trend of fecal butyric acid compared to labeled butyric acid, which was added prior to sample collection as stability standards. This inconsistency could likely arise due to the adsorption of the spiked standards (including other undetected spiked standards) onto the walls of the vials during drying. This may make it potentially difficult to redissolve them, especially considering that the vials are filled with fecal homogenates. Another potential limitation is the collection by trained staff (volunteers). For instance, using noncommercial 95% ethanol kits for sampling may present practical challenges compared to using commercial kits such as OMNIgene•GUT. In the current study, trained staff conducted the sampling; however, the effectiveness of using 95% EtOH for lay study participants for home collection needs to be tested. Notwithstanding this, the ongoing Alzheimer's Gut Microbiome Project (<https://alzheimergut.org/>) has already tested the feasibility of using 95% EtOH. It is also worth noting that all subjects in this study were adults, and the metabolite and microbiome content of feces differ in different age ranges, such as in children. Therefore, further validation may be necessary to test fecal samples collected from a wider range of age groups. Another factor that limits the reliability of

fecal sample collection is the variability in the volume and weight of the feces (water and fiber content). To address this, in the current setting, we collected fecal samples volumetrically, using a weight-to-volume ratio of 1:4 (weight of feces to volume of ethanol 95%) to match the W:V ratio in the commercially available kit OMNIgene•GUT. Notwithstanding that, two steps may be taken to address this issue. First, the collection tube (95% ethanol kits) should be weighed before it is sent to the participant to obtain an accurate measurement of the fecal sample weight. Second, participants report their stool consistency, which is strongly associated with the composition of the gut microbiota and metabolite content. By considering dry weight, we may be able to account for the physicochemical bias during the sample collection process. In terms of microbiome profiling, our study was limited to metatranscriptomics (i.e., 16S rRNA gene sequencing) analyses, and future studies should consider metagenomics (whole shotgun metagenomic sequencing) and study if 95% EtOH collection is suitable for metatranscriptomics (gene expression study).

## CONCLUSIONS

Overall, our study found that storing feces samples at room temperature and stabilizing them in OMNImet•GUT or 95% EtOH yielded metabolomic results generally comparable to flash freezing. Specifically, we observed similar identities and abundances of detected biochemicals as well as comparable metabolic profiles of the study subjects. Moreover, we characterized metabolic changes in crude feces over time, which could be attributed to microbiota activity and nonenzymatic reactions such as oxidation–reduction. Therefore, samples could be reasonably stored in these examined preservatives at room temperature for up to 7 days. Utilizing 95% EtOH as a fecal collection matrix can offer a more convenient and cost-effective way to collect and store feces samples at home. Individual differences in microbiome's overall composition dominated those of the storage type. However, OMNIgene•GUT was slightly better than 95% EtOH at preserving microbiota based on  $\alpha$  diversity. Further exploration of an existing commercial kit is ongoing and will expand the microbiome and metabolome assessment.

## ASSOCIATED CONTENT

### Supporting Information

The Supporting Information is available free of charge at <https://pubs.acs.org/doi/10.1021/acs.analchem.3c04436>.

List of targeted metabolites including GLCA, GCDCA, GDCA, GCA, and several unknown metabolites (ZIP)

Additional Methods section; ASCA results from endocannabinoids, lipids, and untargeted metabolomics data; plots showing concentration levels of endocannabinoids and lipids over time (24, 36, 48 h, 7 days); and  $\alpha$  and  $\beta$  diversity results (PDF)

## AUTHOR INFORMATION

### Corresponding Authors

Rima Kaddurah-Daouk – Department of Psychiatry and Behavioral Sciences, Duke University, Durham, North Carolina 27708-0187, United States;  
Email: [rima.kaddurahdaouk@duke.edu](mailto:rima.kaddurahdaouk@duke.edu)

Alex M. Dickens – Turku Bioscience Centre, University of Turku, 20520 Turku, Finland; Department of Chemistry,

University of Turku, 20500 Turku, Finland; [orcid.org/0000-0002-3178-8449](https://orcid.org/0000-0002-3178-8449); Email: [alex.dickens@utu.fi](mailto:alex.dickens@utu.fi)

Santosh Lamichhane – Turku Bioscience Centre, University of Turku, 20520 Turku, Finland; [orcid.org/0000-0002-9292-3595](https://orcid.org/0000-0002-9292-3595); Email: [santosh.lamichhane@utu.fi](mailto:santosh.lamichhane@utu.fi)

## Authors

Heidi Isokääntä – Research Center for Infections and Immunity, Institute of Biomedicine, University of Turku, 20520 Turku, Finland

Lucas Pinto da Silva – Turku Bioscience Centre, University of Turku, 20520 Turku, Finland

Naama Karu – Metabolomics and Analytics Centre, Leiden Academic Centre for Drug Research, Leiden University, Leiden 2333 CC, The Netherlands

Teemu Kallonen – Department of Clinical Microbiology, Laboratory Division, Turku University Hospital, 20520 Turku, Finland; Clinical Microbiome Bank, Microbe Center, University Hospital and University of Turku, 20520 Turku, Finland

Anna-Katariina Aatsinki – Centre for Population Health Research, University of Turku, 20520 Turku, Finland

Thomas Hankemeier – Metabolomics and Analytics Centre, Leiden Academic Centre for Drug Research, Leiden University, Leiden 2333 CC, The Netherlands

Leyla Schimmel – Department of Psychiatry and Behavioral Sciences, Duke University, Durham, North Carolina 27708-0187, United States

Edgar Diaz – Department of Psychiatry and Behavioral Sciences, Duke University, Durham, North Carolina 27708-0187, United States

Tuulia Hyötyläinen – School of Science and Technology, Örebro University, 70281 Örebro, Sweden; [orcid.org/0000-0002-1389-8302](https://orcid.org/0000-0002-1389-8302)

Pieter C. Dorrestein – Center for Microbiome Innovation, University of California, San Diego, La Jolla, California 92093-6607, United States; Collaborative Mass Spectrometry Innovation Center, Skaggs School of Pharmacy and Pharmaceutical Sciences, University of California, San Diego, La Jolla, California 92093-0657, United States;  
[orcid.org/0000-0002-3003-1030](https://orcid.org/0000-0002-3003-1030)

Rob Knight – Center for Microbiome Innovation, University of California, San Diego, La Jolla, California 92093-6607, United States

Matej Orešič – Turku Bioscience Centre, University of Turku, 20520 Turku, Finland; School of Medical Sciences, Faculty of Medicine and Health, Örebro University, 702 81 Örebro, Sweden

Complete contact information is available at:

<https://pubs.acs.org/10.1021/acs.analchem.3c04436>

## Notes

The authors declare the following competing financial interest(s): Dr. Kaddurah-Daouk is an inventor on a series of patents on the use of metabolomics for the diagnosis and treatment of CNS diseases and holds equity in Metabolon Inc., Chymia LLC and PsyProtix.

## ACKNOWLEDGMENTS

The authors thank the Turku Metabolomics Center for the assistance and resources in the analysis of fecal metabolome and lipidome. The authors thank Matilda Kråkström for her excellent support in the technical details of the metabolomics

analysis and Päivi Haaranen for her technical support in NGS library preparation. The authors also thank Henok Karvonen for his assistance with the graphical abstract. This study was supported by the National Institute on Health grant (U19AG063744; PI: Kaddurdah-Daouk) and the Academy of Finland project grant, (No. 323171 to S.L.), (No. 333981 to M.O.), Swedish Research Council (Grant No. 2016-05176 to T.H. and M.O.), Formas (Grant No. 2019-00869 to T.H. and M.O.), and the Novo Nordisk Foundation (Grant No. NNF20OC0063971 to T.H. and M.O.). Further support was received from “Inflammation in human early life: targeting impacts on life-course health” (INITIALISE) consortium funded by the Horizon Europe Program of the European Union under Grant Agreement 101094099 (to M.O. and T.H.) and Alzheimer’s Gut Microbiome Project (<https://alzheimergut.org/>). A.A. and H.I. were supported by the Signe and Ane Gyllenberg Foundation (grant no. 6273). H.I. received funding from the Finnish Cultural Foundation (grant no. 00230482) and further supported by the Doctoral Program in Clinical Research at the University of Turku. Funding sources had no role in study design, the collection, analysis, and interpretation of data, the writing of the report, or in the decision to submit the article for publication. All authors approved the final version and had final responsibility for the decision to submit for publication.

## REFERENCES

- (1) Visconti, A.; Le Roy, C. I.; Rosa, F.; Rossi, N.; Martin, T. C.; Mohny, R. P.; Li, W.; de Rinaldis, E.; Bell, J. T.; Venter, J. C.; Nelson, K. E.; Spector, T. D.; Falchi, M. *Nat. Commun.* **2019**, *10* (1), No. 4505.
- (2) Sommer, F.; Bäckhed, F. *Nat. Rev. Microbiol.* **2013**, *11* (4), 227–238.
- (3) Gomaa, E. Z. *Antonie van Leeuwenhoek* **2020**, *113* (12), 2019–2040.
- (4) Fan, Y.; Pedersen, O. *Nat. Rev. Microbiol.* **2021**, *19* (1), 55–71.
- (5) Franzosa, E. A.; Sirota-Madi, A.; Avila-Pacheco, J.; Fornelos, N.; Haiser, H. J.; Reinker, S.; Vatanen, T.; Hall, A. B.; Mallick, H.; McIver, L. J.; Sauk, J. S.; Wilson, R. G.; Stevens, B. W.; Scott, J. M.; Pierce, K.; Deik, A. A.; Bullock, K.; Imhann, F.; Porter, J. A.; Zhernakova, A.; Fu, J.; Weersma, R. K.; Wijmenga, C.; Clish, C. B.; Vlamakis, H.; Huttenhower, C.; Xavier, R. J. *Nat. Microbiol.* **2019**, *4* (2), 293–305.
- (6) Muscogiuri, G.; Cantone, E.; Cassarano, S.; Tuccinardi, D.; Barrea, L.; Savastano, S.; Colao, A. *Int. J. Obes. Suppl.* **2019**, *9* (1), 10–19.
- (7) Cryan, J. F.; O’Riordan, K. J.; Cowan, C. S. M.; Sandhu, K. V.; Bastiaanssen, T. F. S.; Boehme, M.; Codagnone, M. G.; Cusotto, S.; Fulling, C.; Golubeva, A. V.; Guzzetta, K. E.; Jaggar, M.; Long-Smith, C. M.; Lyte, J. M.; Martin, J. A.; Molinero-Perez, A.; Moloney, G.; Morelli, E.; Morillas, E.; O’Connor, R.; Cruz-Pereira, J. S.; Peterson, V. L.; Rea, K.; Ritz, N. L.; Sherwin, E.; Spichak, S.; Teichman, E. M.; van de Wouwe, M.; Ventura-Silva, A. P.; Wallace-Fitzsimons, S. E.; Hyland, N.; Clarke, G.; Dinan, T. G. *Physiol. Rev.* **2019**, *99* (4), 1877–2013.
- (8) Sorboni, S. G.; Moghaddam, H. S.; Jafarzadeh-Esfehani, R.; Soleimanpour, S. *Clin. Microbiol. Rev.* **2022**, *35* (1), No. e0033820.
- (9) Ursell, L. K.; Haiser, H. J.; Van Treuren, W.; Garg, N.; Reddivari, L.; Vanamala, J.; Dorrestein, P. C.; Turnbaugh, P. J.; Knight, R. *Gastroenterology* **2014**, *146* (6), 1470–1476.
- (10) Wang, Z.; Zolnik, C. P.; Qiu, Y.; Usyk, M.; Wang, T.; Strickler, H. D.; Isasi, C. R.; Kaplan, R. C.; Kurland, I. J.; Qi, Q.; Burk, R. D. *Front. Cell. Infect. Microbiol.* **2018**, *8*, No. 301.
- (11) Zierer, J.; Jackson, M. A.; Kastenmüller, G.; Mangino, M.; Long, T.; Telenti, A.; Mohny, R. P.; Small, K. S.; Bell, J. T.; Steves, C. J.; Valdes, A. M.; Spector, T. D.; Menni, C. *Nat. Genet.* **2018**, *50* (6), 790–795.
- (12) Stevens, V. L.; Hoover, E.; Wang, Y.; Zanetti, K. A. *Metabolites* **2019**, *9* (8), 156.
- (13) Ramamoorthy, S.; Levy, S.; Mohamed, M.; Abdelghani, A.; Evans, A. M.; Miller, L. A. D.; Mehta, L.; Moore, S.; Freinkman, E.; Hourigan, S. K. *BMC Microbiol.* **2021**, *21* (1), No. 59.
- (14) Lim, M. Y.; Hong, S.; Kim, B. M.; Ahn, Y.; Kim, H. J.; Nam, Y. D. *Sci. Rep.* **2020**, *10* (1), No. 1789.
- (15) Lofftfield, E.; Vogtmann, E.; Sampson, J. N.; Moore, S. C.; Nelson, H.; Knight, R.; Chia, N.; Sinha, R. *Cancer Epidemiol. Biomarkers Prev.* **2016**, *25* (11), 1483–1490.
- (16) Ingram, L. O. *Crit. Rev. Biotechnol.* **1989**, *9* (4), 305–319.
- (17) de Goffau, M. C.; Jallow, A. T.; Sanyang, C.; Prentice, A. M.; Meagher, N.; Price, D. J.; Revill, P. A.; Parkhill, J.; Pereira, D. I. A.; Wagner, J. *Nat. Microbiol.* **2022**, *7* (1), 132–144.
- (18) Williams, G. M.; Leary, S. D.; Ajami, N. J.; Chipper Keating, S.; Petrosin, J. F.; Hamilton-Shield, J. P.; Gillespie, K. M. *PLoS One* **2019**, *14* (6), No. e0216557.
- (19) Kråkström, M.; Dickens, A. M.; Alves, M. A.; Forssten, S. D.; Ouwehand, A. C.; Hyötyläinen, T.; Orešič, M.; Lamichhane, S. *Metabolites* **2023**, *13* (3), No. 355.
- (20) Pluskal, T.; Castillo, S.; Villar-Briones, A.; Oresic, M. *BMC Bioinf.* **2010**, *11*, No. 395.
- (21) Bolyen, E.; Rideout, J. R.; Dillon, M. R.; Bokulich, N. A.; Abnet, C. C.; Al-Ghalith, G. A.; Alexander, H.; Alm, E. J.; Arumugam, M.; Asnicar, F.; Bai, Y.; Bisanz, J. E.; Bittinger, K.; Brejnrod, A.; Brislawn, C. J.; Brown, C. T.; Callahan, B. J.; Caraballo-Rodríguez, A. M.; Chase, J.; Cope, E. K.; Da Silva, R.; Diener, C.; Dorrestein, P. C.; Douglas, G. M.; Durall, D. M.; Duvallet, C.; Edwardson, C. F.; Ernst, M.; Estaki, M.; Fouquier, J.; Gauglitz, J. M.; Gibbons, S. M.; Gibson, D. L.; Gonzalez, A.; Gorlick, K.; Guo, J.; Hillmann, B.; Holmes, S.; Holste, H.; Huttenhower, C.; Huttley, G. A.; Janssen, S.; Jarmusch, A. K.; Jiang, L.; Kaehler, B. D.; Kang, K. B.; Keefe, C. R.; Keim, P.; Kelley, S. T.; Knights, D.; Koester, I.; Kosciolk, T.; Kreps, J.; Langille, M. G. I.; Lee, J.; Ley, R.; Liu, Y. X.; Lofftfield, E.; Lozupone, C.; Maher, M.; Marotz, C.; Martin, B. D.; McDonald, D.; McIver, L. J.; Melnik, A. V.; Metcalf, J. L.; Morgan, S. C.; Morton, J. T.; Naimey, A. T.; Navas-Molina, J. A.; Nothias, L. F.; Orchanian, S. B.; Pearson, T.; Peoples, S. L.; Petras, D.; Preuss, M. L.; Pruesse, E.; Rasmussen, L. B.; Rivers, A.; Robeson, M. S., 2nd; Rosenthal, P.; Segata, N.; Shaffer, M.; Shiffer, A.; Sinha, R.; Song, S. J.; Spear, J. R.; Swafford, A. D.; Thompson, L. R.; Torres, P. J.; Trinh, P.; Tripathi, A.; Turnbaugh, P. J.; Ul-Hasan, S.; van der Hoof, J. J. J.; Vargas, F.; Vázquez-Baeza, Y.; Vogtmann, E.; von Hippel, M.; Walters, W.; Wan, Y.; Wang, M.; Warren, J.; Weber, K. C.; Williamson, C. H. D.; Willis, A. D.; Xu, Z. Z.; Zaneveld, J. R.; Zhang, Y.; Zhu, Q.; Knight, R.; Caporaso, J. G. *Nat. Biotechnol.* **2019**, *37* (8), 852–857.
- (22) Lamichhane, S.; Yde, C. C.; Jensen, H. M.; Morovic, W.; Hibberd, A. A.; Ouwehand, A. C.; Saarinen, M. T.; Forssten, S. D.; Wiebe, L.; Marcussen, J.; Bertelsen, K.; Meier, S.; Young, J. F.; Bertram, H. C. *J. Proteome Res.* **2018**, *17* (3), 1041–1053.
- (23) Nogal, A.; Valdes, A. M.; Menni, C. *Gut Microbes* **2021**, *13* (1), 1–24.
- (24) Lamichhane, S.; Sen, P.; Alves, M. A.; Ribeiro, H. C.; Raunio, P.; Hyötyläinen, T.; Orešič, M. *Metabolites* **2021**, *11* (1), 55.
- (25) Brown, E. M.; Ke, X.; Hitchcock, D.; Jeanfavre, S.; Avila-Pacheco, J.; Nakata, T.; Arthur, T. D.; Fornelos, N.; Heim, C.; Franzosa, E. A.; Watson, N.; Huttenhower, C.; Haiser, H. J.; Dillow, G.; Graham, D. B.; Finlay, B. B.; Kostic, A. D.; Porter, J. A.; Vlamakis, H.; Clish, C. B.; Xavier, R. J. *Cell Host Microbe* **2019**, *25* (5), 668–680.e7.
- (26) Lee, M. T.; Le, H. H.; Johnson, E. L. *J. Lipid Res.* **2021**, *62*, No. 100034.
- (27) Guan, H.; Pu, Y.; Liu, C.; Lou, T.; Tan, S.; Kong, M.; Sun, Z.; Mei, Z.; Qi, Q.; Quan, Z.; Zhao, G.; Zheng, Y. *mSphere* **2021**, *6* (5), No. e0063621.

(28) Chen, L.; Zhernakova, D. V.; Kurilshikov, A.; Andreu-Sánchez, S.; Wang, D.; Augustijn, H. E.; Vich Vila, A.; Weersma, R. K.; Medema, M. H.; Netea, M. G.; Kuipers, F.; Wijmenga, C.; Zhernakova, A.; Fu, J. *Nat. Med.* **2022**, *28* (11), 2333–2343.

(29) Zhu, A.; Sunagawa, S.; Mende, D. R.; Bork, P. *Genome Biol.* **2015**, *16* (1), No. 82.

(30) Gilbert, J. A. *Genome Biol.* **2015**, *16* (1), No. 97.

(31) Jones, J.; Reinke, S. N.; Ali, A.; Palmer, D. J.; Christophersen, C. T. *Sci. Rep.* **2021**, *11* (1), No. 13964.

(32) Trošt, K.; Ahonen, L.; Suvitaival, T.; Christiansen, N.; Nielsen, T.; Thiele, M.; Jacobsen, S.; Krag, A.; Rossing, P.; Hansen, T.; Dragsted, L. O.; Legido-Quigley, C. *Sci. Rep.* **2020**, *10* (1), No. 885.

(33) Millspaugh, J. J.; Washburn, B. E. *Gen. Comp. Endocrinol.* **2003**, *132* (1), 21–26.

(34) Lamichhane, S.; Sundekilde, U. K.; Blædel, T.; Dalsgaard, T. K.; Larsen, L. H.; Dragsted, L. O.; Astrup, A.; Bertram, H. C. *Anal. Methods* **2017**, *9* (30), 4476–4480.